Available online at www.sciencedirect.com

jmr&t
Journal of Materials Research and Technology

journal homepage: www.elsevier.com/locate/jmrt

Original Article

Development of boron doped diamond electrodes material for heavy metal ion sensor with high sensitivity and durability

Shin Kim [a,1], *Yesul Jeong* [a,1], *Min-Ouk Park* [b], *Yujin Jang* [a], *Jong-Seong Bae* [a], *Kyong-Soo Hong* [a], *Seohan Kim* [c,d], *Pungkeun Song* [e,**], *Jang-Hee Yoon* [a,*]

[a] *Busan Center, Korea Basic Science Institute (KBSI), Busan, South Korea*
[b] *Technology Research Institute, Suntech Engineering Co., Ltd., Daegu, South Korea*
[c] *Material Technology Research Institute, Pusan National University, Busan, South Korea*
[d] *Department of Materials Science and Engineering, The Ångström Laboratory, Uppsala University, SE-75103 Uppsala, Sweden*
[e] *Department of Material Science and Engineering, Pusan National University, Busan, South Korea*

ARTICLE INFO

Article history:
Received 5 September 2022
Accepted 17 January 2023
Available online 22 January 2023

Keywords:
Boron doped diamond
Environmental chemistry
Electrodes of anodic stripping voltammetry
Heavy metal detection sensors
Water quality monitoring

ABSTRACT

We report on the optimized substrate pretreatment and deposition process conditions for boron-doped diamond (BDD) electrodes fabricated by hot-filament chemical vapor deposition (HFCVD). The optimized BDD electrode with a doping concentration of 8000 ppm showed high accuracy and precision in detecting Cd(II), Pb(II), and Cu(II) ions. In addition, this demonstrates excellent selectivity against external metal ions under the optimized stripping voltammetry measurement conditions. The detection limits of the target ions of Cd(II), Pb(II), and Cu(II) were 0.55 (±0.05), 0.43 (±0.04), and 0.74 (±0.06) μg/L (S/N = 3), respectively. In real samples spiked with 100 μg/L Cd(II), Pb(II), and Cu(II), both the accuracy and precision of the BDD electrode were within 5%; the interference with organic matter was also negligible. The excellent selectivity and long-term stability indicate that the BDD electrode developed in this study are potentially useful for online water environment monitoring systems.

* Corresponding author.
** Corresponding author.
E-mail addresses: pksong@pusan.ac.kr (P. Song), jhyoon@kbsi.re.kr (J.-H. Yoon).
[1] These authors contributed equally to this work.

https://doi.org/10.1016/j.jmrt.2023.01.116

1. Introduction

Industrial wastewater containing various heavy metal ions has been discharged in increasingly large quantities with the recent increase in industrial development [1–5]. Exposure to high levels of trace metal ions (e.g., Cd(II), Pb(II), and Cu(II)) causes a variety of health and environmental problems. These toxic species, when accumulated in the human body through water sources, have a low rate of clearance [2,4,6]. To minimize human exposure to these contaminants through effective water quality monitoring, spectroscopic [7,8] and electroanalytical [9–13] techniques are widely used. Most spectroscopic methods use expensive large-scale equipment and require regular sampling and long analysis times [14,15]. In comparison, electroanalytical techniques are easy to use in situ for measurements in rivers and lakes as they involve apparatus that can be easily handled. Electroanalysis also enables rapid and continuous measurements and is relatively inexpensive compared to spectroscopic detection methods.

The anodic stripping voltammetry (ASV) method is mainly used for the electrochemical detection of heavy metal ions. The ASV method has a wide linear dynamic range, a low detection limit on the order of parts per billion (ppb), multi-element analysis capability, and simple instrumentation that is relatively inexpensive, small in size, low in electrical power requirements, and sufficiently portable for field use [16–18]. Therefore, ASV has been used successfully for the determination of heavy metal content in water. The sensitivity of differential-pulse polarography is higher than those of other classical polarography methods, because of the enhanced faradaic current and reduced non-faradaic charging current.

In general, Hg is used as the electrodes in the ASV method for detecting trace heavy metal ions; however, Hg electrodes are both toxic and volatile [16]. Many studies on heavy metal detection sensors such as modified glassy carbon (GC) [19,20], diamond [21–23], and Au [24,25] have been conducted to improve electrochemical performance while maintaining environmental friendliness. Among them, boron-doped diamond (BDD) electrodes have been tested for use in detecting trace heavy metal ions because they feature good electrical conductivity, low background current, and are non-toxic [16]. The BDD electrode, which behaves as a p-type semiconductor when B is doped into diamond, has the mechanical properties of diamond as well as excellent electrical properties. In addition, it has excellent electrochemical stability, a wide potential window [26,27], and excellent selectivity and repeatability in heavy metal ion detection [28]. Because of these advantages, much research has been conducted for various applications related to the environment, such as heavy metal detection sensors [29–33] and wastewater electrolysis [26,34–36] using BDD electrodes.

Although BDD electrodes have excellent electrochemical performance, there are many issues that are yet to be addressed. For example, BDD electrodes are not suitable for commercial applications because of the difficulties in process optimization and the high manufacturing costs involved in the processing of gases and substrate materials. Furthermore, many working electrodes, including BDD electrodes, used in conventional three-electrode electrochemical measurements are sampled by cutting into small sizes and molding with epoxy to avoid exposing the outside of the measurement surface. These types of electrodes, namely the so-called disk electrodes, are inconvenient with regard to sampling, as they require steps such as applying an Ag paste and fixing Cu contacts. In addition, the measurement solution can permeate the space between the electrode and the epoxy and cause measurement noise. Currently, studies on the development of flat substrate-based BDD electrodes using hot-filament chemical vapor deposition (HFCVD) are conducted to improve the convenience and speed of heavy metal detection.

The optimization of the process condition of HFCVD is key to improving the electrochemical performance of the BDD electrodes [37–39]. This is because the inappropriate doping concentration of B in diamond leads to poor crystal growth and electrical properties, which result in low detection sensitivity and accuracy. There have been few studies on process development for the fabrication of BDD electrodes [40–42]. However, a detailed understanding of the improvements in electrochemical performance by controlling the B content doped in the diamond during processing is particularly lacking.

In this study, the fabrication condition of BDD electrodes on Si substrates using HFCVD was optimized by controlling the B doping concentration. The differential-pulse ASV (DPASV) method was applied for the simultaneous electrochemical detection of the Cd(II), Pb(II), and Cu (II) species of multiple heavy metal ions. Through the optimization of the processing and DPASV measurement conditions, we increased the detection sensitivity for heavy metal ions. The BDD electrodes were then applied for sensing detection on a real sample.

2. Experimental

2.1. Preparation of electrodes

A B-doped diamond layer was deposited on a polycrystalline Si substrate (100 × 100 × 5 mm) by HFCVD. The optimal deposition conditions derived from previous studies on improving the adhesion of the BDD electrode layer were used. To remove impurities from the surface of the substrate and to improve the adhesion of the diamond layer, the three steps of sanding, etching, and seeding were performed before deposition. Thereafter, the oven-dried sample was placed in a chamber, and a reactive gas comprising hydrogen, methane, and trimethyl borate (TMB) was injected to deposit a BDD electrode layer. The process pressure was 51 Torr, the substrate–filament distance was 15 mm, and the processing temperature was approximately 1200 °C. The BDD electrode samples were prepared with TMB gas flow ratios of 100, 700, 2500, 5000, 8000, and 10,000 ppm, which changed the B doping concentrations. The BDD electrode was deposited for 10 h, resulting in a thickness of 2.5–3 μm, and a sample was prepared by laser-cutting the electrode to a size of 20 × 50 mm for application in a self-made electrochemical cell.

2.2. Characterization

The surface morphologies of the BDD electrodes were observed by high-resolution scanning electron microscopy

Table 1 – Comparison of BDD electrode with other reported methods in terms of sensor performance.

Electrode	Method	Linear range (μg/L)	Detection limit (μg/L)	Ref.
BDD	DPASV	5–100	Cd(II): 3.5 Pb(II): 2.0 Cu(II): 0.1	[13]
BDD	DPASV	Cd(II): 3.2–70 Pb(II): 7.7–100 Cu(II): 7.7–100	Cd(II): 1 Pb(II): 2.3 Cu(II): 2.3	[19]
BDD	DPASV		Cd(II): 2.47 Pb(II): 51.5	[24]
BDD	SWASV	Cd(II): 5.6–448 Pb(II): 10.3–1648	Cd(II): 3.39 Pb(II): 3.62	[40]
BDD	DPASV	1–1000	Cd(II): 0.55 ± 0.05 Pb(II): 0.43 ± 0.04 Cu(II): 0.74 ± 0.06	This work

(HR-SEM, SU-70, Hitachi, Japan). The chemical bonding states and B doping contents of the electrode surfaces were observed using an X-ray photoelectron spectrometer (XPS, K-ALPHA+, Thermo Scientific, USA) with a monochromatic Al Kα source including charge compensation at the Korea Basic Science Institute (KBSI) (Busan, South Korea). Raman spectra were observed at the KBSI using a confocal Raman imaging spectrometer (XperRam 200, AsiaAnalytics, Taiwan). X-ray diffractometry (XRD, X'Pert PRO, Malvern PANalytical, UK) was used to determine the deposited metal phases at KBSI. The thicknesses of the BDD electrodes and the diffusion behaviors of the elements were confirmed at the KBSI using a glow-discharge spectrometer (GDS, JY 10000RF, HORIBA Jobin Yvon, France). Qualitative and quantitative analyses of heavy metal ions in real samples were confirmed at the KBSI using an inductively coupled plasma atomic emission spectrophotometer (ICP-AES, ACTIVA S, HORIBA Jobin Yvon, France).

2.3. *Measurement of electrochemical sensitivity of the electrodes towards the heavy metal ion*

As a buffer solution, 0.1-M acetate buffer was used, with the pH adjusted by mixing 0.1-M sodium acetate (Sigma-Aldrich Co., USA) with 0.1-M acetic acid solution (Sigma-Aldrich Co., USA). A standard heavy metal ion solution containing 100 ppm each of Cd(II), Pb(II), and Cu(II) was purchased from AccuStandard Inc. (USA). Aqueous solutions diluted to 1, 10, 50, 100, 250, 500, and 1000 ppb were prepared by mixing the standard solution with appropriate amounts of the 0.1-M acetate buffer solution. A 0.1-M H_2SO_4 solution diluted with distilled water was also prepared for activation of the electrode surfaces. In addition, high-purity (99.999%) N_2 gas was used to remove bubbles from the electrode surface during the measurement. All aqueous solutions were prepared with distilled water using a Milli-Q water-purifying system (18 MΩ cm).

The presence of heavy metal ions causes changes in the current, potential, electrochemical impedance, capacitance, or electrochemiluminescence of the system; these changes can be used for ion detection [43]. We used a potentiostat (KST P-1, Kosentech, South Korea) to confirm the electrochemical sensitivity of the electrodes to heavy metal ions by the DPASV method. The BDD electrodes, Ag/AgCl (saturated KCl), and Pt wire were used as the WE, RE, and CE, respectively. Fig. 1 and Fig. S1 show a schematic diagram of a handmade polytetrafluoroethylene three-electrode electrochemical cell for electrochemical analysis of a flat BDD electrodes (20 × 50 × 5 mm) [44]. This cell, which uses flat working electrodes, enables continuous electrochemical measurement, resulting in high efficiency and improved convenience. In addition, the memory effect, which was a problem of traditional disk electrodes, was also solved by using an electrochemical cell (Fig. S2).

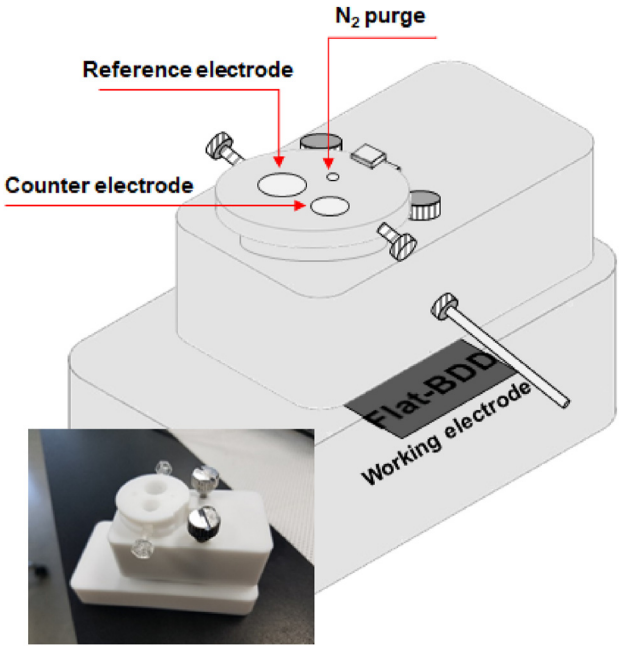

Fig. 1 – Schematic of handmade electrochemical cell for electrochemical analysis of a flat plat BDD electrode.

Electrochemical stabilization was performed using cyclic voltammetry (CV) to remove the adsorption layer, impurities, and electrochemical activation of surface from the electrode surface before heavy metal detection. First, using a 0.1-M H_2SO_4 solution, 10 CV cycles were performed at a scan rate of 250 mV/s at a potential range −2.0 to 2.0 V to activate a wide

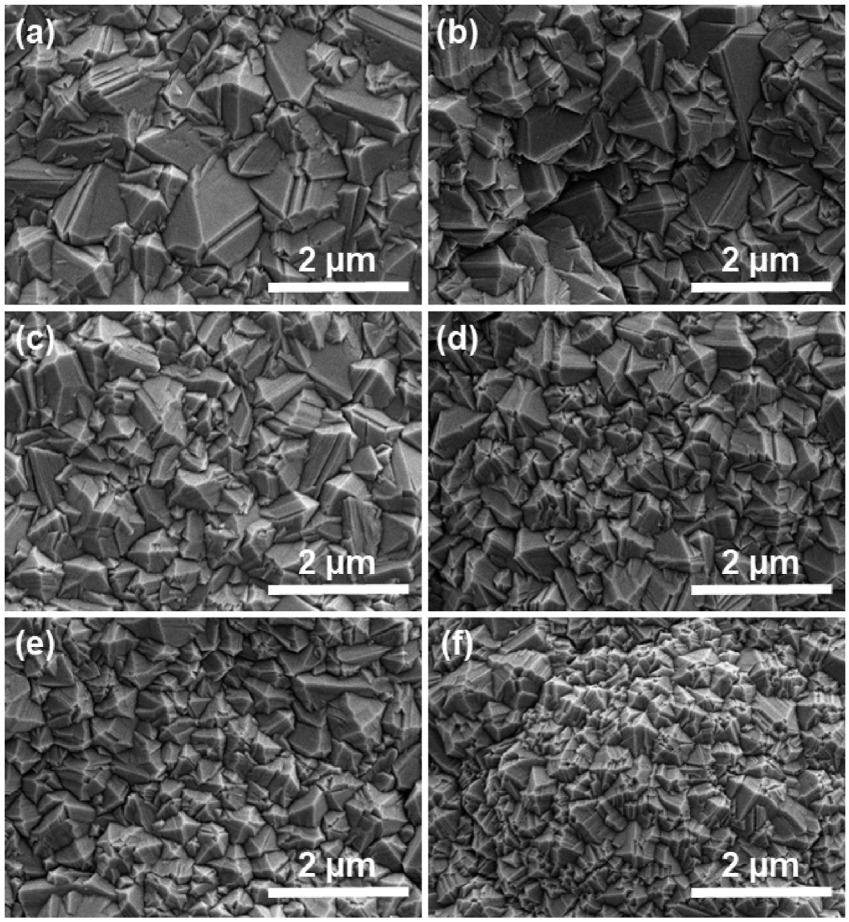

Fig. 2 – Comparison of surface morphologies of BDD electrodes with different B doping concentrations as determined by the TMB flow ratio during deposition.

range of electrode potentials. Secondly, 10 CV cycles were performed under the same conditions at −1.5 to 1.5 V with a 0.1-M acetate buffer solution for heavy metal ion analysis and residual solution washing. Distilled water was used for all experimental procedures and solution washing, and the electrode surface was dried using an air gun.

3. Results and discussion

3.1. *Optimization of B doping concentration for BDD electrodes*

The surface characteristics of the BDD electrodes (in terms of the B doping concentration during fabrication) were investigated using HR-SEM, XPS, Raman spectroscopy, and GDS.

Fig. 2 shows the HR-SEM images of the surface shapes of the BDD electrodes. With the increase in B doping concentration from 100 to 10,000 ppm during deposition, the size of the diamond crystals in the electrode changes. This is caused by the increase in amount of B atoms that are substituted when entering the diamond lattice with the increased TMB gas flow ratio. It should be noted that the BDD electrode with TMB gas flow ratios of 8000 ppm possesses a dense grain structure and an even surface, as shown in Fig. 2(e). Meanwhile, the BDD electrode fabricated with a TMB gas flow ratio of 10,000 ppm exhibited a noticeable defective grain, uneven grain size, and a rough surface, resulting from the re-extraction of B atoms due to over-doping.

To confirm B doping in the diamond crystals, XPS spectra of the BDD electrode fabricated with various TMB gas flows are presented in Fig. 3. As shown by the XPS spectra, the TMB flow ratio-dependent B doping content increases for flow ratios up to 8000 ppm and then decreases for flow ratios greater than 10,000 ppm. This influences the increase in crystal size up to 8000 ppm, as shown in Fig. 2(e). However, at 10,000 ppm, internal distortion of the diamond lattice occurs with the over-doping of B atoms. Consequently, the substituted B atoms are then re-extracted, affecting the crystallinity and electrical conductivity.

In the Raman spectra (Fig. 4), a 1332 cm^{-1} and ~520 cm^{-1} are observed, which is related to B doping in diamond film [41,45]. When the doping rate is increased, both peaks shift to a lower wavenumber and become broader and weaker by showing peaks at ~500 cm^{-1} and ~1200 cm^{-1}. This indicates that the B atoms are well doped into the diamond lattice with the increase in the B doping content, resulting in a decrease in the sp3/sp2 ratio [46]. Meanwhile, a diamond-like carbon (DLC)

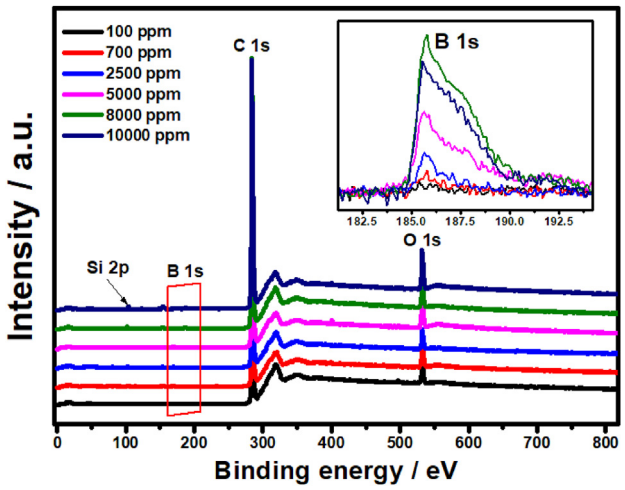

Fig. 3 – XPS spectra of BDD electrodes with different B doping concentrations as determined by the TMB gas flow ratio during deposition.

layer or carbide formation increases the lattice mismatch between the substrate and the diamond layer, which is the main cause of decreased adhesion [37,46]. However, carbide formation can be properly controlled by adjusting the B content, which leads to further decrease in the sp3/sp2 ratio and increase in the electrochemical properties [46]. The XRD pattern (Fig. S3) shows the formation of a carbide layer due to the diffusion of the substrate material into the BDD electrode, which improves the detection sensitivity for heavy metal ions [45,47]. Therefore, the results presented here indicate that appropriate BDD electrodes can be fabricated by HVCVD by controlling the B doping concentration. In addition, our study shows an optimum B doping concentration, i.e., 8000 ppm.

Fig. 5 shows the GDS depth profile of the BDD electrode deposited at the TMB flow ratio of 8000 ppm. The thickness of the BDD electrode deposited for 6 h using HFCVD is about 2.5 μm. This electrode is a pure BDD layer with no diffused Si within 600 nm of the surface. At depths greater than 600 nm, the material can be classified as a diffusion BDD layer in which carbide, diamond, and B atoms are well mixed by diffusion of the substrate up to around 2.5 μm in depth. B atoms are relatively more concentrated at the surface; the concentration gradually decreases to a minimum at ~2.5 μm.

3.2. *Optimization of analytical parameters*

Fig. 6 shows the results of optimizing the DPASV measurement conditions to evaluate the electrochemical properties of the electrode using a BDD sample with the optimized B concentration. The measurement conditions of the supporting electrolyte, pH, molar concentration, and deposition time are optimized for the simultaneous detection of Cd(II), Pb(II), and Cu(II) ions, as shown in Fig. 6. Differences in current changes are observed for each supporting electrolyte. After adding 1 ppm each of the three species Cd(II), Pb(II), and Cu(II) to a 0.1-M acetate buffer, 0.1-M KCl, and 0.1-M KNO_3, the effects of the supporting electrolytes on the current value are compared. The change in the current is the highest in the system with the 0.1-M acetate buffer. Fig. 6(b) shows the detection sensitivities for the three heavy metal ions according to changes in the pH (3.5–5.5) of the 0.1-M acetate buffer. The highest detection sensitivity is achieved at pH 5.0. When performing measurements on the BDD electrode, it is determined that a weakly acidic environment is advantageous for surface activation and measurement. Next, the detection sensitivities according to changes in the molar concentration (0.05–0.20 M) of the acetate buffer electrolyte at a pH of 5.0 are examined. The highest detection sensitivity is achieved in the 0.1-M acetate buffer. Fig. 6(d) shows the detection sensitivities toward the three heavy metal species according to the electrodeposition time using the DPASV method. The resting time before electrodeposition is 5 s. By adjusting the electrodeposition time between 0 and 300 s, it is determined that the detection sensitivities for the three heavy metal species are the highest

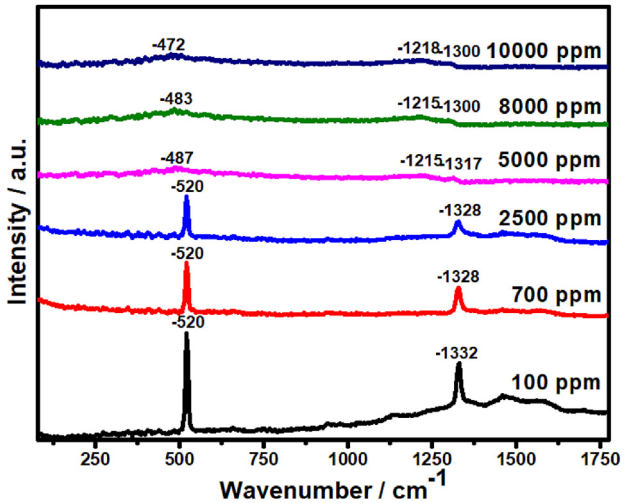

Fig. 4 – Raman spectra of BDD electrodes in relation to B doping concentration as determined by the TMB flow ratio during deposition.

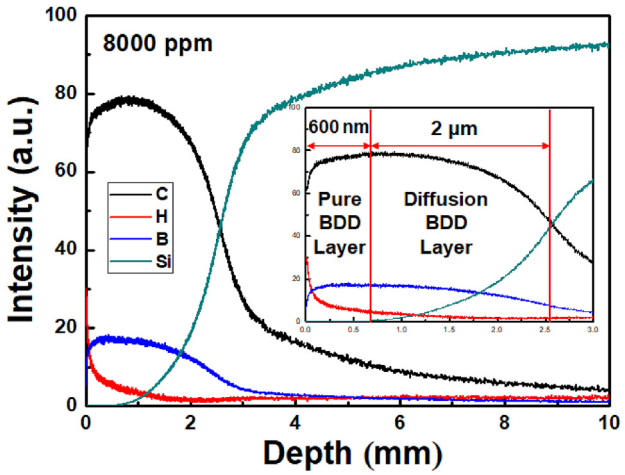

Fig. 5 – GDS depth profile of BDD electrode with optimized B doping concentration with deposition at a TMB flow ratio of 8000 ppm.

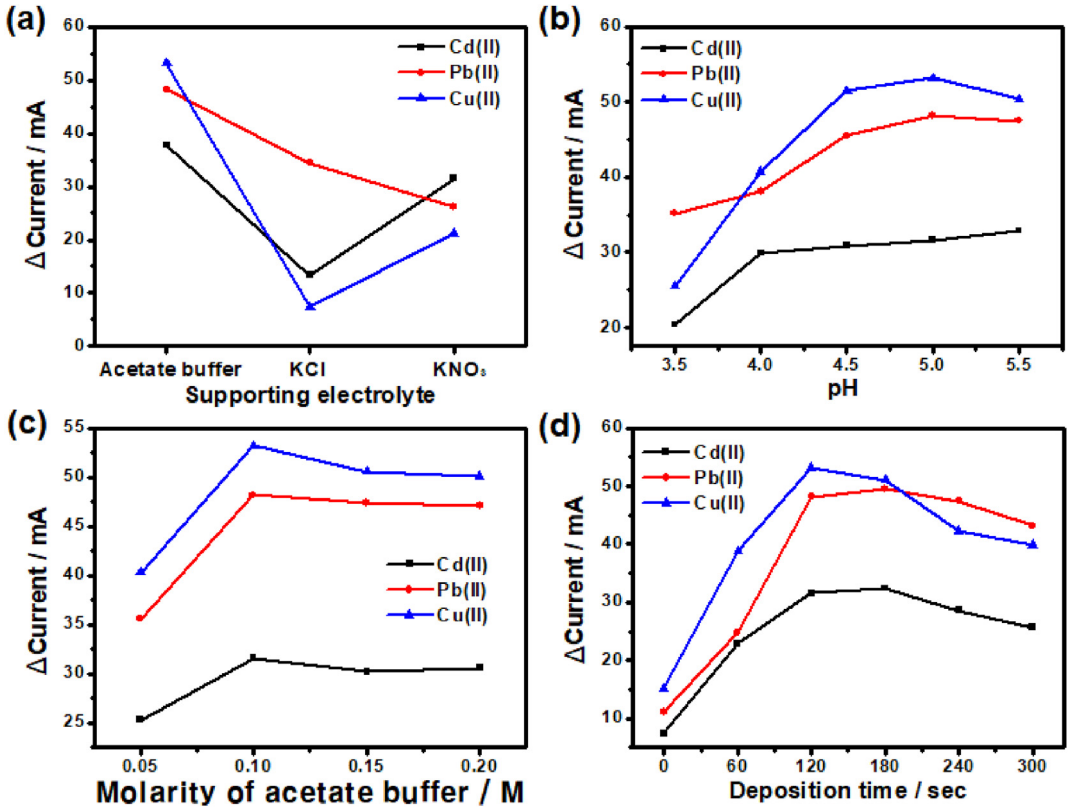

Fig. 6 – Optimization of measurement conditions for DPASV measurement. (a) Supporting electrolyte, (b) pH of 0.1-M acetate buffer (c) electrolyte molarity, (d) electrodeposition time.

with a deposition time of 120 s. Higher deposition times yield decreased detection sensitivities; this is attributed to an interference effect by heavy metal ions unnecessarily adsorbed on the electrode surface. Additionally, the analytical parameters affecting the DPASV response for detection of 1000 ppb of Cd(II), Pb(II), and Cu(II) were optimized by considering (A) the pulse amplitude and (B) the scan rate (Fig. S4). The effect of amplitude on the detection sensitivity was investigated between 10 and 100. As the pulse amplitude increased, the detection sensitivity of Cd(II), Pb(II), and Cu(II) also increased. Fig. S4(b) shows the effect of scan rate on the detection sensitivity of 1000 ppb Cd(II), Pb(II), and Cu(II). The detection sensitivity of Cd(II), Pb(II), and Cu(II) increased up to a scan rate of 250 mV/s but decreased at 300 mV/s. This is considered to be due to the adsorption of heavy metal ions on the electrode because of the fast stripping potential. Therefore, the final supporting electrolyte conditions are a 0.1 M acetate buffer at a pH of 5.0 with an electrodeposition time of 120 s, a pulse amplitude of 100 mV, and a scan rate of 250 mV/s. These conditions are used in subsequent experiments.

3.3. *Analytical performance*

Fig. 7 shows the simultaneous detection sensitivities for Cd(II), Pb(II), and Cu(II) according to the B doping concentration of the BDD electrodes. In DPASV measurements, the pulse amplitude was 100 mV, the scan rate was 250 mV/s, the electrodeposition time was 120 s, the measurement range was −1.5–1.5 V, and Cd(II), Pb(II), and Cu(II) heavy metals of 1 ppm each of were measured in a 0.1-M acetate buffer. The detection sensitivity of the three heavy metals tended to increase as the TMB gas flow ratio during electrode deposition was increased from 100 to 8000 ppm. The highest detection

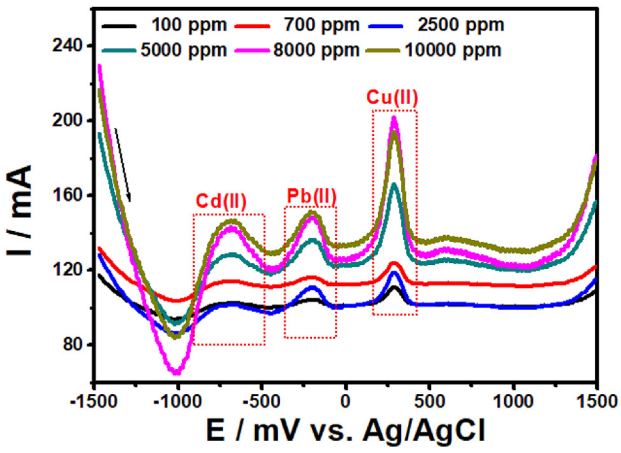

Fig. 7 – Comparison of Cd(II), Pb(II), and Cu(II) detection sensitivities of BDD electrodes with different B doping concentrations achieved by varying the TMB gas flow ratio during deposition.

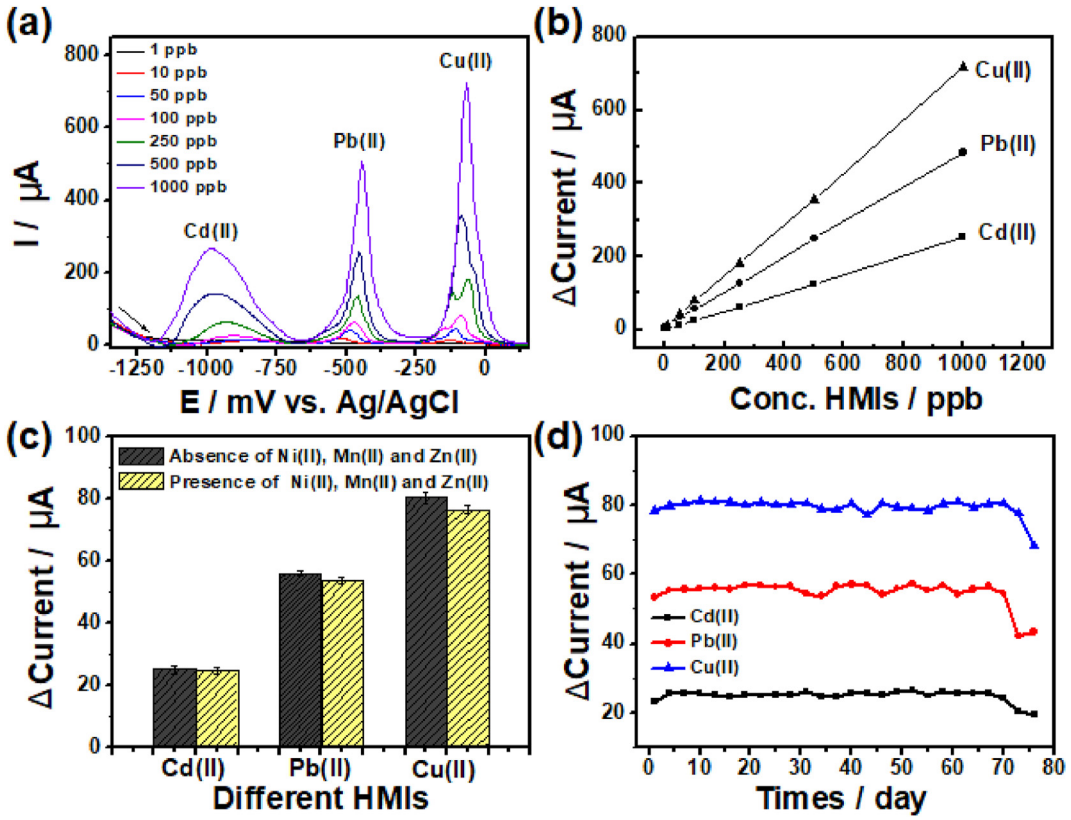

Fig. 8 – Analytical performance evaluation using optimized BDD electrode and DPASV measurement conditions. (a) Voltammograms of Cd(II), Pb(II), and Cu(II) ions, (b) calibration plot of Cd(II), Pb(II), and Cu(II) (heavy metal ions, HMIs) concentrations from 1 to 1000 ppb, (c) interference effects by other heavy metal ions (HMIs) at 300 ppb each, (d) long-term stability of BDD electrode.

sensitivity was achieved for the electrode formed with 8000-ppm TMB; the sensitivity for the BDD electrode deposited with an increased TMB flow ratio of 10,000 ppm was reduced. Because the detection sensitivity of the BDD electrode fabricated with a TMB flow ratio of 8000 ppm was the highest under the same measurement conditions, this was set as the optimum concentration. Additionally, the detection sensitivity of Cu(II) is the highest because of the excellent electrical conductivity of Cu. Under the same electrodeposition time, Cu, which has the relatively good conductivity, causes more ions to be electrodeposited and detached from the electrode surface. As a result, a quantitative difference is observed compared with amount of Cd(II) and Pb(II) ions. This is consistent with other studies on heavy metals multi detection reported [48–51].

The voltammogram and calibration plot measured using the electrode with the optimized B doping concentration and the optimized DPASV method are shown in Fig. 8(a) and (b), respectively. The solution used for calibration was diluted in a 0.1-M acetate buffer of pH 5.0 with Cd(II), Pb(II), and Cu(II) standard solutions within the range of 1 ppb–1000 ppb. A total of seven points were measured. The shoulder peak separation during oxidation is observed in Cu(II), which is mainly resulted in the influence of Cu ions ligands [52–54]. Due to the reduction potential, Cu^{2+} ion is electrodeposited on electrode surface as the state of metallic Cu(0). During oxidation, this is oxidized to the Cu(II) and Cu(I) ligands, which causes peak separation of Cu^{2+} and Cu^{1+}. This phenomenon depends on the experimental conditions such as the type and concentration of electrolytes and electrodeposition condition, and other studies have reported complex formation of copper ligands using this phenomenon [55,56]. The peaks of Cd(II), Pb(II), and Cu(II) tended to shift with an increase in concentration, which is believed to be because of the changes in pH accompanying the ionic concentration changes. However, Cd(II), Pb(II), and Cu(II) showed distinct peaks at all concentrations within the potential ranges of −987 to −900 mV, −520 to −440 mV, and −127 to −67 mV, respectively. The linear dynamic range for the three heavy metal species ranged from 1 μg/L to 1000 μg/L, and the detection limits of Cd(II), Pb(II), and Cu(II) for five repeated measurements were derived to be 0.55 (±0.05), 0.43 (±0.04), and 0.74 (±0.06) μg/L (S/N = 3), respectively. The relative standard deviation (RSD) values for Cd(II), Pb(II), and Cu(II) were 1.64, 1.44, and 2.22%, respectively, indicating excellent precision within 5%. These results should be compared with other reports on sensor performance using BDD electrodes, which are summarized in Table 1. As an example, Tall et al. examined a BDD electrode for heavy metal detection using the DPASV method [23]. Compared with a glassy carbon electrode, the BDD electrode in this study showed detection and

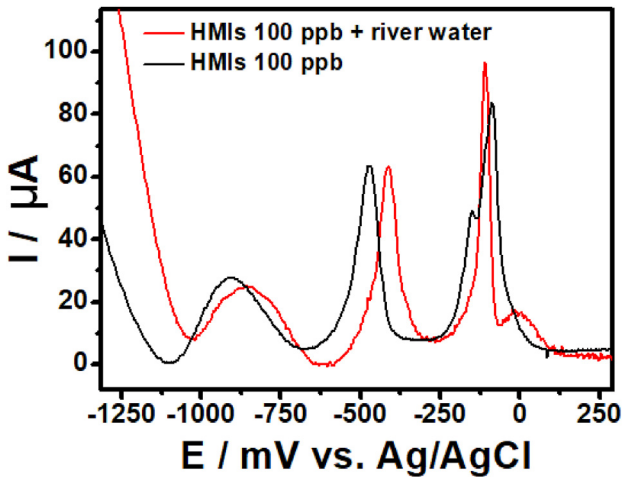

Fig. 9 – Analysis of a real sample of Daegu Seongseo river water spiked to 100 ppb using BDD electrode.

sensitivity values that were four and two times higher, respectively. However, it should be noted that the sensing properties of the BDD electrodes in our study were significantly higher than those in Ref. [23] as indicated by the detection limits of 1 μg/L, 2.3 μg/L, and 2.3 μg/L for Cd(II), Pb(II), and Cu(II), respectively. On the other hand, in another study, the SWASV method were adopted for the simultaneous detection of Cd(II) and Pb(II) using BDD electrodes [57]. Good detection performance was achieved by the electrodes fabricated using the optimized process parameters in this study compared to that of mercury film electrodes; however, this performance was still considerably lower than that of our BDD electrodes. Therefore, the excellent sensing performance of the BDD electrodes developed in our study demonstrates their potential for use in online monitoring systems in a water environment.

To evaluate the selectivity of the BDD electrode, Mn(II), Ni(II), and Zn(II) were added to the Cd(II), Pb(II), and Cu(II) solutions to investigate the interference effects of external metal ions. Fig. 8(c) shows the interference effects of external metal ions with 3 ppm each of Mn(II), Ni(II), and Zn(II) under the optimized measurement conditions. The detection sensitivities for Cd(II), Pb(II), and Cu(II) ions decreased by 2.12, 4.1, and 4.7%, respectively, when other metal ions were added at concentrations of 3.0 ppm or more. However, Ni(II), Mn(II), and Zn(II) ions added at concentrations of 100 ppb, equal to those of Cd(II), Pb(II), and Cu(II), did not significantly affect the detection sensitivities.

Fig. 8(d) depicts the long-term stability as measured through repeated tests using a BDD electrode with the optimized B doping concentration. After the currents of solutions with added Cd(II), Pb(II), and Cu(II) were measured and confirmed against the current of the blank solution, a clean blank curve without residual adsorbed ions was obtained after washing the used electrode with distilled water. Measurements following this cycle were performed three times a day using 100-ppb Cd(II), Pb(II), and Cu(II) solutions for more than 70 days. The average detection sensitivities for Cd(II), Pb(II), and Cu(II) ions decreased by 4.78, 3.84, and 1.99%, respectively, over 65 days. During the evaluation period, it was confirmed that the change in the current value was maintained at a maximum of 95% or more, and that the BDD electrode could be used stably and continuously to measure Cd(II), Pb(II), and Cu(II).

3.4. *Real sample*

An experiment was conducted to measure the concentrations of Cd(II), Pb(II), and Cu(II) in a real sample using the BDD electrode with the optimized B concentration and the optimum measurement conditions. The real sample used for the measurement was a river water sample obtained from the Seongseo area in Daegu, South Korea. A standard for spiking was made by diluting Cd(II), Pb(II), and Cu(II) ions to concentrations of 100 ppb.

Fig. 9 compares the detection sensitivity of the electrode for the 100-ppb standard to those measured for river water spiked with 100 ppb of the HMI species. Unlike the curve of the 100-ppb standard, that of the spiked river water sample appears to have peaks corresponding to organic matter. ICP-AES analysis shows that Cu at a concentration of 50 ppb is present in the river water, and Cu at a concentration of approximately 25 ppb is present in the river water diluted 1:1 with 0.1-M acetate buffer for DPASV measurement. For the standard addition method, 100 ppb of standard Cd(II), Pb(II), and Cu(II) solutions were added to the river water sample; the concentration values obtained through the voltammogram of Cd(II), Pb(II), and Cu(II) were 97.85, 100.71, and 124.99 ppb, respectively. This result indicates no significant difference between the ICP-AES results and the sensor results. Similar results are obtained for the 50 ppb and 250 ppb of Cd(II), Pb(II), and Cu(II) in a real sample (for details, see Supplementary data, Fig. S5). The BDD electrode used in the experiment is therefore suitable for the simultaneous detection of Cd(II), Pb(II), and Cu(II) in real samples, showing excellent accuracy with negligible interference by organic matter.

4. Conclusion

We optimized the substrate pretreatment process and HFCVD process to develop a BDD electrode with an optimal B doping concentration for detecting Cd(II), Pb(II), and Cu(II) in water. It was confirmed through Raman spectroscopy and HR-SEM imaging that the B atoms were well doped into the diamond lattice and increasing the B doping concentration did not cause any grain damage. In addition, it was confirmed by XPS spectra that B doping concentration was the highest in the electrode formed by deposition using a TMB gas flow ratio of 8000 ppm. Lattice distortion occurred because of excessively doped B atoms in samples with higher TMB flow ratios of 10,000 ppm; this distortion impaired the crystallinity. The BDD electrode fabricated with a TMB gas flow ratio of 8000 ppm showed excellent selectivity and repeatability for the detection of Cd(II), Pb(II), and Cu(II) ions. It also showed good measurement results without the adsorption of heavy metal ions under the optimized measurement conditions. In addition, the BDD electrode was very stable and sensitive in

detecting Cd(II), Pb(II), and Cu(II). When analyzing a real sample, the electrode showed high accuracy and precision, making it possible to detect Cd(II), Pb(II), and Cu(II) ions without interference effects from various heavy metal ions. The high stability of the electrode was confirmed through repeated long-term measurements. Owing to its excellent properties, the optimized BDD electrode is expected to be applied to various environmental fields such as water environmental monitoring systems.

Declaration of competing interest

The authors declare that they have no known competing financial interests or personal relationships that could have appeared to influence the work reported in this paper.

Acknowledgement

This work was supported by Korea Basic Science Institute grant (grant number C230320), the R&D Center for Green Patrol Technologies through R&D for Global Top Environmental Technologies (grant number 20180018400013), and partially supported by the life waste recycling technology development project (grant number 20190027400012) funded by the Korea Ministry of Environment.

Appendix A. Supplementary data

Supplementary data to this article can be found online at https://doi.org/10.1016/j.jmrt.2023.01.116.

Appendix A

Additional characterization figures and data including schematics of handmade electrochemical cell, memory effect measurement, XRD results and optimization of analytical parameter.

Supplementary material related to this article can be found in the online version at:

REFERENCES

[1] Qdais HA, Moussa H. Removal of heavy metals from wastewater by membrane processes: a comparative study. Desalination 2004;164(2):105–10. https://doi.org/10.1016/s0011-9164(04)00169-9.

[2] Mahipal SS, Rajeev K. Contaminant of heavy metals in groundwater & its toxic effects on human health & environment. Int. J. Environ. Sci. Nat. Res. 2019;18(5):555996. https://doi.org/10.19080/IJESNR.2019.18.555996.

[3] Wu W, Wu P, Yang F, Sun D, Zhang D-X, Zhou Y-K. Assessment of heavy metal pollution and human health risks in urban soils around an electronics manufacturing facility. Sci Total Environ 2018;630:53–61. https://doi.org/10.1016/j.scitotenv.2018.02.183.

[4] Park M-O, Noh H-B, Park D-S, Yoon J-H, Shim Y-B. Long-life heavy metal ions sensor based on graphene oxide-anchored conducting polymer. Electroanalysis 2016;29(2):514–20. https://doi.org/10.1002/elan.201600494.

[5] Saleh TA, Mustaqeem M, Khaled M. Water treatment technologies in removing heavy metal ions from wastewater: a review. Environ Nanotechnol Monit Manag 2022;17:100617. https://doi.org/10.1016/j.enmm.2021.100617.

[6] Li M, Gou H, Al-Ogaidi I, Wu N. Nanostructured sensors for detection of heavy metals: a review. ACS Sustainable Chem Eng 2013;1(7):713–23. https://doi.org/10.1021/sc400019a.

[7] Heath C, Pejcic B, Myers MB. Block copolymer-coated ATR-FTIR spectroscopic sensors for monitoring hydrocarbons in aquatic environments at high temperature and pressure. ACS Appl. Polym. Mater. 2019;1(8):2149–56. https://doi.org/10.1021/acsapm.9b00420.

[8] Shi W, Zhuang W-E, Hur J, Yang L. Monitoring dissolved organic matter in wastewater and drinking water treatments using spectroscopic analysis and ultra-high resolution mass spectrometry. Water Res 2020:116406. https://doi.org/10.1016/j.watres.2020.116406.

[9] Zinoubi K, Majdoub H, Barhoumi H, Boufi S, Jaffrezic-Renault N. Determination of trace heavy metal ions by anodic stripping voltammetry using nanofibrillated cellulose modified electrode. J Electroanal Chem 2017;799:70–7. https://doi.org/10.1016/j.jelechem.2017.05.039.

[10] Aragay G, Pons J, Merkoçi A. Recent Trends in macro-, micro-, and nanomaterial-based tools and strategies for heavy-metal detection. Chem. Rev. 2011;111(5):3433–58. https://doi.org/10.1021/cr100383r.

[11] Novotný V, Barek J. Voltammetric Determination of aclonifen at a silver amalgam electrode in drinking and river water. Ecol. Chem. Eng. S. 2017;24(2):277–84. https://doi.org/10.1515/eces-2017-0019.

[12] Zheng J, Rahim MA, Tang J, Allioux F-M, Kalantar-Zadeh K. Post-transition metal electrodes for sensing heavy metal ions by stripping voltammetry. Adv. Mater. Technol. 2021;7(1):2100760. https://doi.org/10.1002/admt.202100760.

[13] Bayraktepe CYDE, Yazan Z, Önal M. Bismuth nanoparticles decorated on Na-montmorillonite-multiwall carbon nanotube for simultaneous determination of heavy metal ions- electrochemical methods. J Electroanal Chem 2022;910(1):116205. https://doi.org/10.1016/j.jelechem.2022.116205.

[14] Lee S, Bong S, Ha J, Kwak M, Park S-K, Piao Y. Electrochemical deposition of bismuth on activated graphene-nafion composite for anodic stripping voltammetric determination of trace heavy metals, Sens. Actuators B Chem 2015;215:62–9. https://doi.org/10.1016/j.snb.2015.03.032.

[15] Li S, Zhang C, Wang S, Liu Q, Feng H, Ma X, et al. Electrochemical microfluidics techniques for heavy metal ion detection. Analyst 2018. https://doi.org/10.1039/c8an01067f.

[16] Yoon J-H, Yang J, Kim J, Bae J, Shim Y-B, Won M-S. Simultaneous detection of Cd (II), Pb (II), Cu (II), and Hg (II) Ions in dye waste water using a boron doped diamond electrode with DPASV. Bull Kor Chem Soc 2010;31(1). https://doi.org/10.5012/bkcs.2010.31.01.140.

[17] Guo Z, Li D, Luo X, Li Y, Zhao Q-N, Li M, et al. Simultaneous determination of trace Cd(II), Pb(II) and Cu(II) by differential pulse anodic stripping voltammetry using a reduced graphene oxide-chitosan/poly- l -lysine nanocomposite modified glassy carbon electrode. J Colloid Interface Sci 2017;490:11–22. https://doi.org/10.1016/j.jcis.2016.11.006.

[18] El-Desoky HS, Beltagi AM, Ghoneim MM, El-Hadad AI. The first utilization of graphene nano-sheets and synthesized Fe_3O_4 nanoparticles as a synergistic electrodeposition platform for simultaneous voltammetric determination of

some toxic heavy metal ions in various real environmental water samples. Microchem J 2022;175:106966. https://doi.org/10.1016/j.microc.2021.106966.
[19] Palisoc S, Causing AM, Natividad M. Gold nanoparticle/hexaammineruthenium/Nafion® modified glassy carbon electrodes for trace heavy metal detection in commercial hair dyes. Anal Methods 2017;9(29):4240–6. https://doi.org/10.1039/c7ay01114h.
[20] Shah A, Nisar A, Khan K, Nisar J, Niaz A, Ashiq MN, et al. Amino acid functionalized glassy carbon electrode for the simultaneous detection of thallium and mercuric ions. Electrochim Acta 2019:134658. https://doi.org/10.1016/j.electacta.2019.134658.
[21] Deshmukh S, Sankaran KJ, Korneychuk S, Verbeeck J, Mclaughlin J, Haenen K, et al. Nanostructured nitrogen doped diamond for the detection of toxic metal ions. Electrochim Acta 2018;283:1871–8. https://doi.org/10.1016/j.electacta.2018.07.067.
[22] Pei J, Yu X, Zhang Z, Zhang J, Wei S, Boukherroub R. In-situ graphene modified self-supported boron-doped diamond electrode for Pb(II) electrochemical detection in seawater. Appl Surf Sci 2020;527:146761. https://doi.org/10.1016/j.apsusc.2020.146761.
[23] Tall OE, Jaffrezic-Renault N, Sigaud M, Vittori O. Anodic stripping voltammetry of heavy metals at nanocrystalline boron-doped diamond electrode. Electroanalysis 2007;19(11):1152–9. https://doi.org/10.1002/elan.200603834.
[24] Najafzadeh F, Ghasemi F, Hormozi-Nezhad MR. Anti-aggregation of gold nanoparticles for metal ion discrimination: a promising strategy to design colorimetric sensor arrays. Sens. Actuators B Chem. 2018;270:545–51. https://doi.org/10.1016/j.snb.2018.05.065.
[25] Podesva P, Gablech I, Neuzil P. Nanostructured Gold microelectrode array for ultrasensitive detection of heavy metal contamination. Anal Chem 2018;90:1161–7. https://doi.org/10.1021/acs.analchem.7b03725.
[26] Lim PY, Lin FY, Shih HC, Ralchenko VG, Varnin VP, Pleskov YV, et al. Improved stability of titanium based boron-doped chemical vapor deposited diamond thin-film electrode by modifying titanium substrate surface. Thin Solid Films 2008;516(18):6125–32. https://doi.org/10.1016/j.tsf.2007.11.016.
[27] Salvo-Comino C, Rassas I, Minot S, Bessueille F, Rodriguez-Mendez ML, Errachid A, et al. Voltammetric sensor based on electrodeposited molecularly imprinted chitosan film on BDD electrodes for catechol detection in buffer and in wine samples. Mater. Sci. Eng. C. 2020;110:110667. https://doi.org/10.1016/j.msec.2020.110667.
[28] Kondo T. Recent electroanalytical applications of boron-doped diamond electrodes. Curr. Opin. Electrochem. 2022;32:100891. https://doi.org/10.1016/j.coelec.2021.100891.
[29] Zazoua A, Khedimallah N, Jaffrezic-Renault N. Electrochemical determination of Cadmium, lead, and nickel using a polyphenol–polyvinyl chloride—boron-doped diamond electrode. Anal Lett 2017;51(3):336–47. https://doi.org/10.1080/00032719.2017.1310879.
[30] Rehacek V, Hotový I, Marton M, Mikolasek M, Michniak P, Vincze A, et al. Voltammetric characterization of boron-doped diamond electrodes for electroanalytical applications. J Electroanal Chem 2020:114020. https://doi.org/10.1016/j.jelechem.2020.114020.
[31] Rusinek CA, Becker MF, Rechenberg R, Schuelke T. Fabrication and characterization of boron doped diamond microelectrode arrays of varied geometry. Electrochem Commun 2016;73:10–4. https://doi.org/10.1016/j.elecom.2016.10.006.
[32] Štenclová P, Vyskočil V, Szabó O, Ižák T, Š Potocký, Kromka A. Structured and graphitized boron doped diamond electrodes: impact on electrochemical detection of Cd2+ and Pb2+ ions. Vacuum 2019;170:108953. https://doi.org/10.1016/j.vacuum.2019.108953.
[33] Liu Z, Baluchová S, Sartori AF, Li Z, Gonzalez-Garcia Y, Schreck M, et al. Heavily boron-doped diamond grown on scalable heteroepitaxial quasi-substrates: A promising single crystal material for electrochemical sensing applications, Carbon; 201(5); 1229-1240. https://doi.org/10.1016/j.carbon.2022.10.023.
[34] Griesbach U, Zollinger D, Pütter H, Comninellis C. Evaluation of boron doped diamond electrodes for organic electrosynthesis on a preparative scale. J Appl Electrochem 2005;35(12):1265–70. https://doi.org/10.1007/s10800-005-9038-2.
[35] Chen X, Chen G, Gao F, Yue PL. High-performance Ti/BDD electrodes for pollutant oxidation. Environ Sci Technol 2003;37(21):5021–6. https://doi.org/10.1021/es026443f.
[36] Bansal R, Verduzco R, Wong MS, Westerhoff P, Garcia-Segura S. Development of nano boron-doped diamond electrodes for environmental applications. J Electroanal Chem 2022;907(15):116028. https://doi.org/10.1016/j.jelechem.2022.116028.
[37] Kim S, Kim S-H, You M-Y, Yoon J-H, Song P-K. Characteristics of boron-doped diamond electrodes deposited on titanium substrate with TiNx interlayer. Nanosci Nanotechnol Lett 2018;10:722–7. https://doi.org/10.1166/nnl.2018.2649.
[38] Gwon JU, Jang TH, Kim MS, Kim TG, Bae MK. Electrochemical properties and morphology of boron-doped diamond thin films. Mod Phys Lett B 2022;36(16):2242007. https://doi.org/10.1142/S0217984922420076.
[39] Wang R, Peng B, Bai H, Guo Z, Wei Q, Wang K, et al. Morphology, defects and electrical properties of boron-doped single crystal diamond under various oxygen concentration Mater. Letture 2022;322(1):132345. https://doi.org/10.1016/j.matlet.2022.132345.
[40] Marton M, Michniak P, Behul M, Rehacek V, Vojs Stanova A, Redhammer R, et al. Bismuth modified boron doped diamond electrode for simultaneous determination of Zn, Cd and Pb ions by square wave anodic stripping voltammetry: influence of boron concentration and surface morphology. Vacuum 2019;167:182–8. https://doi.org/10.1016/j.vacuum.2019.06.012.
[41] Bogdanowicz R, Fabiańska A, Golunski L, Sobaszek M, Gnyba M, Ryl J, et al. Influence of the boron doping level on the electrochemical oxidation of the azo dyes at Si/BDD thin film electrodes. Diam Relat Mater 2013;39:82–8. https://doi.org/10.1016/j.diamond.2013.08.004.
[42] Ferreira NG, Silva LLG, Corat EJ, Trava-Airoldi VJ. Kinetics study of diamond electrodes at different levels of boron doping as quasi-reversible systems. Diam Relat Mater 2002;11(8):1523–31. https://doi.org/10.1016/s0925-9635(02)00060-2.
[43] Cui L, Wu J, Ju H. Electrochemical sensing of heavy metal ions with inorganic, organic and bio-materials. Biosens Bioelectron 2015;63:276–86. https://doi.org/10.1016/j.bios.2014.07.052.
[44] Bernard M, Deneuville A, Muret P. Non-destructive determination of the boron concentration of heavily doped metallic diamond thin films from Raman spectroscopy. Diam Relat Mater 2004;13:282–6. https://doi.org/10.1016/j.diamond.2003.10.051.
[45] Bernard M, Baron C, Deneuville A. About the origin of the low wave number structures of the Raman spectra of heavily boron doped diamond films. Diam Relat Mater 2004;13:896–9. https://doi.org/10.1016/j.diamond.2003.11.082.
[46] Sun J, Lu H, Lin H, Huang W, Li H, Lu J, et al. Boron doped diamond electrodes based on porous Ti substrates. Mater

Lett 2012;83:112–4. https://doi.org/10.1016/j.matlet.2012.05.044.
[47] Yoon J-H, Jung Y-S, Kim S. Electrochemical cell and system. Korea Patent number 1020906940000. 2020.
[48] Wu HP. Dynamics and performance of fast linear scan anodic stripping voltammetry of Cd, Pb, and Cu using in situ-generated ultrathin mercury films. Anal Chem 1996;68:1639–45. https://doi.org/10.1021/ac950879e.
[49] Kitte SA, Li S, Nsabimana A, Gao W, Lai J, Liu Z, et al. Stainless steel electrode for simultaneous stripping analysis of Cd(II), Pb(II), Cu(II) and Hg(II). Talanta 2019;191:485–90. https://doi.org/10.1016/j.talanta.2018.08.066.
[50] Liu L, Zhang K, Wei Y. A simple strategy for the detection of Cu(II), Cd(II) and Pb(II) in water by a voltammetric sensor on a TC4A modified electrode. New J Chem 2019;43:1544. https://doi.org/10.1039/c8nj05089a.
[51] Nsabimana A, Kitte SA, Fereja TH, Halawa MI, Zhang W, Xu G. Recent developments in stripping analysis of trace metals. Curr. Opin. Electrochem. 2019;17:65–71. https://doi.org/10.1016/j.coelec.2019.04.012.
[52] Boussemar M, Menargues L, Benaim J-Y. Anodic stripping voltammetry of copper in natural waters: a qualitative approach to the additional peak(s) occurrence. Electroanalysis 1993;5:125–33. https://doi.org/10.1002/elan.1140050206.
[53] Lurdes M, GonGalves SS, Sigg L. Influence of the medium on the polarographic behavior of Cu(ll). Electroanalysis 1991;3:553–7. https://doi.org/10.1002/elan.1140030616.
[54] Mlakar M, Culjak I, Branica M. Square-wave voltammetry of copper-phenant hroline-tri butylphosphate complex. Analyst 1994;119:2443–6. https://doi.org/10.1039/an9941902443.
[55] Correia dos Santos MM, Sousa PMP, Modesto AMM, Simões Gonçalves ML. Voltammetric behaviour of copper complexes with cytosine and its Nucleoside. Bioelectrochem Bioenerg 1998;45:267–73. https://doi.org/10.1016/S0302-4598(97)00102-5.
[56] Honeychurch KC, Hawkins DM, Hart JP, Cowell DC. Voltammetric behaviour and trace determination of copper at a mercury-free screen-printed carbon electrode. Talanta 2002;57:565–74. https://doi.org/10.1016/S0039-9140(02)00060-7.
[57] Pei J, Yu X, Zhang C, Liu X. Development of a boron-doped diamond electrode for the simultaneous detection of Cd2+ and Pb2+ in water. Int J Electrochem Sci 2019;14:3393–407. https://doi.org/10.20964/2019.04.19.